N-Z distributions of secondary fragments and the evaporation attractor line

R. J. Charity
Department of Chemistry, Washington University, St. Louis, Missouri 63130
(Received 27 January 1998)

The process of light particle evaporation moves the position of an excited fragment in the chart of nuclides towards a line which will be called the evaporation attractor line. The predicted location of this line is parametrized and the conditions necessary for the secondary fragment distributions to reach this line are discussed. [S0556-2813(98)03208-7]

PACS number(s): 24.60.Dr

In many nuclear reactions, one or more excited primary fragments are formed which decay by the evaporation of nucleons and light clusters. This evaporation process can substantially alter the proton-neutron asymmetry of the initial primary fragments. In a study of complex fragment emission in fusion reactions, the Z values of the detected secondary fragments were measured [1]. In order to estimate the average mass associated with each fragment Z, statistical model calculations were performed varying the assumed Z, A, and excitation energy of the primary fragments. It was noted that at sufficiently large excitation energies, independent of the assumed Z and A of the primary fragments, evaporation models predict that the average location of the secondary fragments in the chart of nuclides is always close to a particular line. The location of this line is mainly determined by competition between proton and neutron evaporation.

For compound nuclei on the neutron-rich side of the line, neutron emission is the most important evaporation mode and this drives the system towards the line. On the neutron-poor side, proton emission is the strongest decay mode and again, this acts to move the decaying system towards the line. This line thus acts as if it is attracting the decaying systems and hence it will be called the evaporation attractor line (EAL). The same concept was referred to as the ''residue corridor'' by Dufour *et al.* [2,3] who indicated that its position is near the line where the ratio of neutron and proton decay widths (Γ_n/Γ_p) is unity. For light systems, the attractor line is coincident with the line of β stability. However, for heavier systems, the larger Coulomb barrier for proton emission pushes this line to the neutron-deficient side of the valley of stability. At the attractor, the neutron and proton driving forces are about equal. A system located on the attractor will tend to follow the attractor down to lower masses until its excitation energy is exhausted.

At lower excitation energies, the only other important light particle decay mode is α particle evaporation. The emission of this particle moves the decaying system almost parallel to the attractor line and thus preserves a memory of system's neutron excess or deficiency. For these low excitation energies, α particle emission is often less probable than neutron and proton evaporation and only slows down the general movement towards the attractor.

The calculations and conclusions of Ref. [1] were confined to region of lighter fragments ($Z<40$). The location of the EAL in this region of the chart of nuclides was subsequently found to be coincident with the EPAX formula of Sümmerer *et al.* [4] giving the average location of fragmentation products produced in reactions of GeV protons on target nuclei located close to the line of β stability. These products can therefore be understood as the evaporation residues associated with the decay of highly excited primary fragments produced by the initial reaction with the proton [4].

In light of these conclusions and the need to estimate the mass of fragments with larger Z values, evaporation calculations were performed to cover all of the known region of the chart of nuclides. The conclusions from these calculations are identical to those obtained early apart from two exceptions. First for primary fragments that are very neutron-rich relative to the EAL, the location of the secondary fragments approaches, but never reaches, the attractor line even for very large excitation energies. Also it was determined that for heavier nuclei, the EAL and the EPAX formula for fragmentation products are no longer identical. These two results are related and easily understood (see later).

Statistical model calculations were performed with the computer code GEMINI [5,6]. Apart from the dominant low-energy decay modes (n, p, and α emission), the calculations also consider the evaporation of ground and excited states ($E^*<5$ MeV) of all He, Li, and Be isotopes. Separation energies were obtained from the experimental and predicted masses tabulated in Ref. [7]. The other parameters used in these calculations are identical to those used in Ref. [8].

The location of the evaporation attractor line is determined from evaporation characteristics of the system near the end of its decay path, it is not sensitive to uncertainties in the values of the statistical model parameters at the highest excitation energies. However, these parameters are important when predicting the mass distributions of the fragments. The EAL is sensitive to neutron and proton separation energies, however, except for very heavy systems, the attractor line lies in a region where atomic mass excesses are well known experimentally. The EAL is also sensitive to the Coulomb barriers for proton emission. A number of studies have suggested that average Coulomb barriers for charged particle emission are lower than those obtained from optical model fits (Ref. [8], and references therein). However, at present it is not clear whether this is only a high excitation energy phenomenon or to the extent to which the evaporation of,

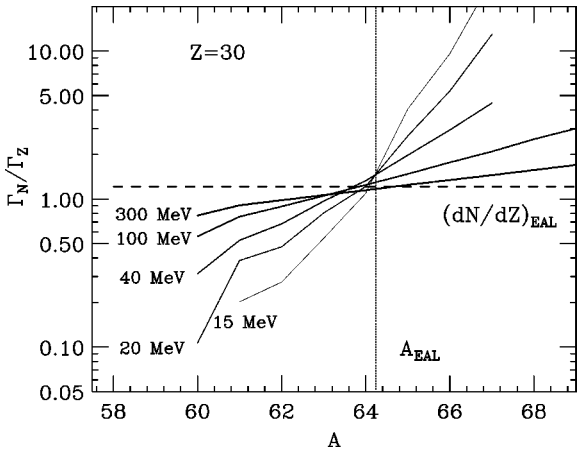

FIG. 1. The ratio Γ_N/Γ_Z predicted by the statistical model calculations for Zn isotopes as a function of mass number. Results are shown for the indicated excitation energies. The position and slope of the attractor line are indicated by the dotted and dashed lines, respectively.

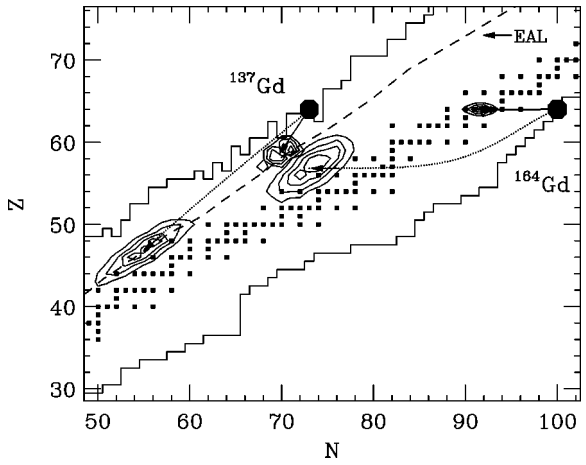

FIG. 2. Contours showing the distribution of secondary fragments in the chart of nuclides predicted for ^{137}Gd and ^{164}Gd compound nuclei with 100 and 400 MeV of excitation energy. The contour interval is 20% of the peak yield. The location of the compound nuclei is indicated by the solid points and the average trajectories followed by the decaying systems are indicated by the solid and dotted curves for the 100 and 400 MeV simulations, respectively. The dashed curve shows the predicted location of the evaporation attractor line (EAL).

and subsequent decay of, unstable clusters can lead to an apparent lowering the Coulomb barriers [8]. Finally, the location of the EAL was found to be largely insensitive to the level density parameter and to the angular momentum of the primary fragment.

The evaporation attractor line obtained from the GEMINI calculations can be well approximated for $Z<90$ by

$$Z=0.909N-1.12\times10^{-3}N^2 \tag{1}$$

or

$$N=1.072Z+2.32\times10^{-3}Z^2. \tag{2}$$

Shell effects cause small deviations, of order of a nucleon or less, to these smooth parametrizations. Note, the present parametrization can be used for heavier systems unlike the one from Ref. [1] which is valid only for $Z<40$.

A more general definition of the attractor can be obtained from the condition

$$\frac{dN}{dZ}=\left\langle\frac{\Gamma_N}{\Gamma_Z}\right\rangle, \tag{3}$$

where Γ_N and Γ_Z are partial decay widths for neutron and proton removal including both the contribution from nucleon and cluster evaporation. At low excitation energy these can be approximated as

$$\Gamma_N=\Gamma_n+2\Gamma_\alpha \tag{4}$$

and

$$\Gamma_Z=\Gamma_p+2\Gamma_\alpha. \tag{5}$$

The contributions from other clusters need to be included at higher excitation energies. As an example, the ratio Γ_N/Γ_Z is plotted as a function of mass number for Zn isotopes in Fig. 1. The curves showing the ratio at different excitation energies all cross close to the intersection of the dotted and dashed lines which indicate the position and slope of the EAL from Eq. (2). Thus at the EAL, the ratio Γ_N/Γ_Z is largely excitation energy independent and has a value appropriate so that, on average, a decaying system stays on the line. In Eq. (3), the EAL is defined in terms of a local average of Γ_N/Γ_Z as shell effects are responsible for local fluctuation in this ratio. The slope of a curve in Fig. 1 gives a measure of the ''restoring force'' which tries to hold the decaying system near the attractor line. For example, if Γ_N/Γ_Z is close to unity, the decaying system moves approximately parallel to the EAL and so does not move towards it or away from it. However, the more the ratio differs from unity, the more direct is movement in N-Z space of the decaying system towards the attractor line. Clearly this ''restoring force'' is reduced at the higher excitation energies. This point will be become very important in the remainder of this paper.

The path by which a decaying fragment approaches the EAL depends on its initial proton-neutron asymmetry and the excitation energy. Typical examples simulated with the GEMINI code are shown in Fig. 2. The contours show the predicted location of secondary fragments produced from the decay of a very neutron-rich ($A=164$) and a very neutron-deficient ($A=137$) Gd compound nucleus. The solid curves show average trajectories followed by the decaying systems when the initial excitation energy is 100 MeV. The neutron-rich system ^{164}Gd is quite distant from the evaporation attractor, and decays towards it almost exclusively by neutron emission. The neutron-deficient system ^{137}Gd is on the other side of the attractor. As it is relatively close to the attractor, its decay is not exclusively by proton emission, there is still some small contribution from neutron emission. However, on average, more protons are emitted and the decaying system moves closer to the attractor.

At higher excitation energies, there is a change in the initial direction of the trajectories in N-Z space. As the nuclear temperature rises, the difference between the energies required to remove a proton and to remove a neutron

(separation energy plus Coulomb barrier) becomes less important and so the rates for proton and neutron emission become more similar. Also, the emission of α particles, deuterons, tritons, and intermediate mass fragments becomes more important. Both of these effects conspire to force the initial trajectories towards paths where, on average, equal number of protons and neutrons are lost and the system retains a memory of its degree of neutron or proton richness. This change in average trajectories is clearly seen in Fig. 2 where the dotted trajectories were predicted for initial excitation energies of 400 MeV. The initial directions of the trajectories for excitation energies of 100 and 400 MeV are quite different. These dotted curves also show that as the systems cool, the forces which drive the decaying system towards the evaporation attractor again become dominant. However, for the neutron-rich system, the average position of the secondary fragments never reaches the evaporation attractor line. As substantial movement towards the attractor only occurs at the lower temperatures, there is a limited number of evaporation steps available during this phase. Therefore if a system is initially located too far from the attractor line, it will move towards, but not reach, the attractor even at very large excitation energies. In principle, the average position of the residue is predicted to slowly approach the EAL as the excitation energy is increased more and more. However, if one is restricted to excitation energies where the model is valid, i.e., where the temperature of the initial system is not greater than the nucleon separation energy, then the very neutron-rich systems such as the ^{164}Gd example will not decay all the way to the attractor line. As the attractor is located closer to proton-rich side of the region of known nuclides, proton-rich fragments will always decay to the EAL, if given enough excitation energy.

One modification to the statistical model calculations which was considered is the predicted temperature dependence of the symmetry energy associated with the change in the effective nucleon mass in the surface of a nucleus [9]. The predicted increase in the symmetry energy at large temperatures will shift the β valley of stability closer to $N=Z$ and so might enhance neutron and reduce proton emission. The kinetic part of the symmetry energy can be related to the temperature dependence of the level density parameter [8]. Calculations employing these modifications were found to have very little affect on the N-Z distributions of the secondary fragments. Basically, the predicted changes in separation energies were always found to be small compared to the temperature and hence has little affect on the predicted particle emission rates. Unless the symmetry energy has a much larger temperature dependence than assumed, this effect can be ignored in statistical model calculations.

Figure 3 gives a general overview of the final position of secondary fragments in the chart of nuclides as a function of initial compound nucleus excitation energy and neutron-proton asymmetry. A selection of compound nuclei which are very neutron-rich, very neutron-deficient, and intermediate examples were calculated with the GEMINI code. The large solid points indicate the position of the selected compound nuclei in the chart of nuclides. The curves extending from these points are the loci of the predicted, average N and Z of the secondary fragments as the excitation energy is increased. The small points indicate the average position of the secondary fragments as the excitation energy is increased in increments of 100 MeV. These curves should not be confused with the average trajectories of the decaying systems which, as shown in Fig. 2, can be quite different at high excitation energies.

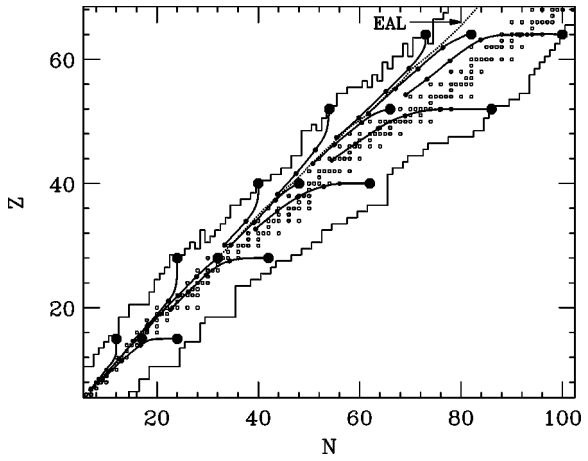

FIG. 3. The curves show the loci of the predicted, average locations of secondary fragments in the chart of nuclides for the compound nuclei indicated by the large solid points. The small points on these curves correspond to the average location of secondary fragments as the excitation energy is increased in 100 MeV increments. The evaporation attractor line (EAL) is indicated.

These curves clearly show that, except for the very neutron-rich fragments, all secondary fragments are found in the vicinity of the evaporation attractor line for large excitation energies. Generally, there is an initial rapid movement towards the attractor when the excitation energy is of the order 100–200 MeV. Once there is enough excitation energy to bring the secondary fragments close to the attractor, increasing the excitation energy only causes the average position to approach the attractor asymptotically, following it down to lower masses. In this excitation energy regime, the secondary fragment N-Z distribution can be described as a ridge orientated parallel to the attractor line (e.g., Fig. 2).

The very neutron-rich systems, as noted early, never reach the evaporation attractor. At high excitation energies the average location of the secondary fragments asymptote to lines approximately parallel to, but on the neutron rich side of the EAL. For the selected neutron-rich compound nuclei shown in Fig. 3, one sees that the final separation from the attractor increases as the mass of the system increases. This is partially a result of the fact that the heavier neutron-rich systems were selected further from the attractor. However, in addition to this selection bias, the increasing separation from the attractor can also be attributed to the shape of the β valley of stability which is broader for larger masses and hence the ''forces'' driving the decaying systems towards the attractor are not as large.

Above $Z \gtrsim 50$, even primary fragments located on the β line of stability are sufficient distance from the EAL that their secondary fragments do not reach the evaporation attractor. To illustrate this, in Fig. 4 the loci of average position of of secondary fragments are shown for selected primary fragments located on the β line of stability. Rather than EAL, the location of the secondary fragments approach and subsequently decay, on average, down the dotted line in Fig.

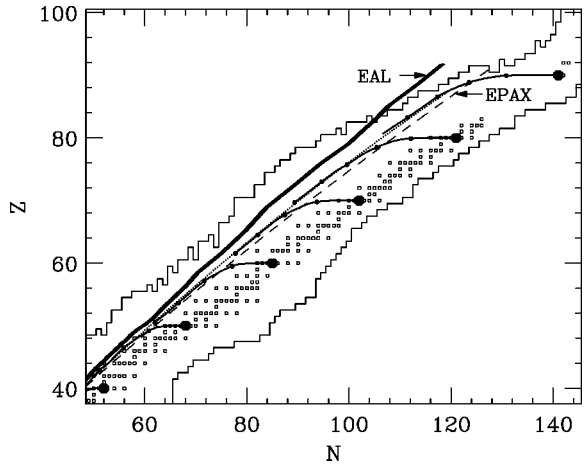

FIG. 4. As in Fig. 3, but now the loci of secondary fragment positions are shown for primary fragments located on the β line of stability. At high excitation energies the final fragment positions follow the dotted curve which is parametrized in the text. For comparison, the EPAX formula is indicated by the dashed line.

4 which can be approximated by the equations

$$Z = 0.911N - 1.50\times 10^{-3}N^2 \tag{6}$$

or

$$N = 1.045Z + 3.57\times 10^{-3}Z^2. \tag{7}$$

From these results it is not surprising that the EPAX formula for the average location of fragmentation products from β stable target nuclei moves away from the evaporation attractor line for large Z. In fact the EPAX formula and the dotted line in Fig. 4 are reasonably similar, and deviate at most by 2 nucleons for the heaviest fragments. Whether or not the EPAX formula and this dotted line should be exactly coincident is not clear, it depends on the neutron richness and excitation energy of the primary products produced in the fragmentation process.

Statistical models calculations were performed varying various model parameters to see if was possible to move the predicted asymptotic line for β stable primary fragments (dotted line in Fig. 4) towards the EPAX parametrization. In this respect is should be noted that for the heavier fragments, the final, low-temperature evaporation sequences are dominated by neutron emission as these fragments are always very neutron-rich compared to the EAL. As such, the location of the asymptotic line for the heavier fragments is not very sensitive to small changes in values of the statistical model parameter at low excitation energies. On the contrary, the values of these parameters at high excitation energy can modify the predicted location of the fragments. It was found that the asymptotic line predicted by GEMINI can be moved to the EPAX parametrization by decreasing the Coulomb barriers for charged particle emission by $\sim$15% or decreasing the level density parameter at high excitation energies to the value $A/16$.

Unlike proton induced target fragmentation, fusionlike reactions between moderately heavy nuclei create compound nuclei on the neutron-deficient side of the valley of stability not too distant from the EAL. Therefore, at large excitation energies, one would expect the secondary fragments to lie along the evaporation attractor line. This has recently been confirmed for the $E/A=14$ and 21 MeV ^{96}Mo+^{58}Ni reactions [10].

Another important property of the EAL is that the average position of secondary fragments can only approach the attractor, but not cross it. This observation can be useful in formulating possible reaction scenarios responsible for the creation of the primary fragments. For example, in a number of studies of projectile fragmentation [11,12] and fusionlike reactions [13] very neutron-deficient nuclei were observed or inferred. However, in the projectile fragmentation studies, the projectile is on the opposite side of the EAL to the detected fragment. Similarly in the fusion study, the compound nucleus and the inferred position of the evaporation residues are on different sides of the evaporation attractor line. As the average decay trajectories of the evaporating fragments cannot cross the EAL, these results cannot be explained in terms of the standard theory of evaporation from the projectile or compound nucleus. In general, the production of such neutron-deficient secondary fragments would seem to require an initial reaction mechanism which produces very neutron-rich primary fragments (on the neutron-rich side of the EAL) with not too much excitation energy [12].

In conclusion, it has been shown that the process of evaporation moves the position of a fragment in the chart of nuclides towards a line which has been called the evaporation attractor line (EAL). Provided the primary fragments have sufficient excitation energy and are not located too far form the EAL, the secondary fragments, on average, will be located on the evaporation attractor line and the fragments will have lost memory of their initial neutron richness or neutron-deficiency.

Substantial movement towards the EAL only occurs when the fragments are relatively cool, and hence there are a limited number of evaporation steps possible in this phase. For primary fragments located too far from the evaporation attractor line, the number of evaporation steps in the cool phase is not sufficient for the average secondary fragment position to reach the EAL. For light nuclei, the location of the secondary fragments will always reach the attractor line if given enough excitation, unless the primary fragments are located close to neutron-rich limits of known nuclides. For $Z\gtrsim 50$, the secondary fragments associated with even β stable primary fragments will not reach the attractor line. These observations explain why the EAL and the EPAX parametrization for the location of fragmentation products from reactions of GeV proton on target nuclei located along the β line of stability move apart for heavier masses.

The use of the evaporation attractor line for estimating the average masses of fragments for which only the Z value is measured must be cautioned if $Z\gtrsim 50$. In such cases, if the initial Z and A of the hot primary fragments are not well known, it may be advisable to consider the range of masses between the values associated with the EAL and the EPAX formula.

This work was supported by the Director, Office of High Energy and Nuclear Physics, Nuclear Physics Division of the U.S. Department of Energy under Contract No. DE-FG02-87ER-40316.

[1] R. J. Charity, D. R. Bowman, Z. H. Liu, R. J. McDonald, M. A. McMahan, G. J. Wozniak, L. G. Moretto, S. Bradley, W. L. Kehoe, and A. C. Mignerery, Nucl. Phys. **A476**, 516 (1988).

[2] J. P. Dufour, H. Delagrange, R. Del Moral, A. Fleury, F. Hubert, Y. Llabador, M. B. Mauhourat, K. H. Schmidt, and A. Lleres, Nucl. Phys. **A387**, 157c (1982).

[3] F. Hubert, R. Del Moral, J. P. Dufour, H. Emmermann, A. Fleury, C. Poinot, M. S. Pravikoff, H. Delagrange, and A. Lleres, Nucl. Phys. **A456**, 535 (1986).

[4] K. Sümmerer, W. Brüchle, D. J. Morrissey, M. Schädel, B. Szweryn, and Yang Weifan, Phys. Rev. C **42**, 2546 (1990).

[5] R. J. Charity, M. A. McMahan, G. J. Wozniak, R. J. McDonald, L. G. Moretto, D. G. Sarantites, L. G. Sobotka, G. Guarino, A. Pantaleo, L. Fiore, A. Gobbi, and K. D. Hildenbrand, Nucl. Phys. **A483**, 371 (1988).

[6] R. J. Charity, Computer code GEMINI (unpublished). This code is available via anonymous ftp from wunmr.wustl.edu in directory /pub/gemini.

[7] P. Möller, J. R. Nix, W. D. Myers, and W. J. Swiatecki, At. Data Nucl. Data Tables **59**, 185 (1995).

[8] R. J. Charity, M. Korolija, D. G. Sarantites, and L. G. Sobotka, Phys. Rev. C **56**, 873 (1997).

[9] P. Donati, P. M. Pizzochero, P. F. Bortignon, and R. A. Broglia, Phys. Rev. Lett. **72**, 2835 (1994).

[10] L. G. Sobotka, R. J. Charity, J. F. Dempsey, H. Scheit, and T. Glasmacher (unpublished).

[11] S. J. Yennello, J. A. Winger, T. Antaya, W. Benenson, M. F. Mohar, D. J. Morrissey, N. A. Orr, and B. M. Sherrill, Phys. Rev. C **46**, 2620 (1992).

[12] K. A. Hanold, D. Bazin, M. F. Mohar, L. G. Moretto, D. J. Morrissey, N. A. Orr, B. M. Sherrill, J. A. Winger, G. J. Wozniak, and S. J. Yennello, Phys. Rev. C **52**, 1462 (1995).

[13] M. Gonin, L. Cooke, K. Hagel, Y. Lou, J. B. Natowitz, R. P. Schmitt, S. Shlomo, B. Srivastava, W. Turnal, H. Utsunomiya, R. Wada, G. Nardelli, G. Nebbia, G. Viesti, R. Zanon, B. Fornal, G. Prete, K. Niita, S. Hannuschke, P. Gonthier, and B. Wilkins, Phys. Rev. C **42**, 2125 (1990).